Action Dark Energy (Marseille November 2022)

Curvature effects on the large scale structure of the universe

arXiv:2206.03059, JCAP 2022

Centre de Physique Théorique (CPT)
Julien Bel

Collaborators:
Louis Perenon (*Lead*)
Christian Marinoni
Roy Maartens
Julien Larena

Outline

1) Motivation for studying galaxy clustering in curved space

2) Fourier basis in curved space

3) Galaxy clustering in configuration space

4) Results (KLCDM)

5) Conclusion

Motivation

The example of the cosmic microwave background (CMB):

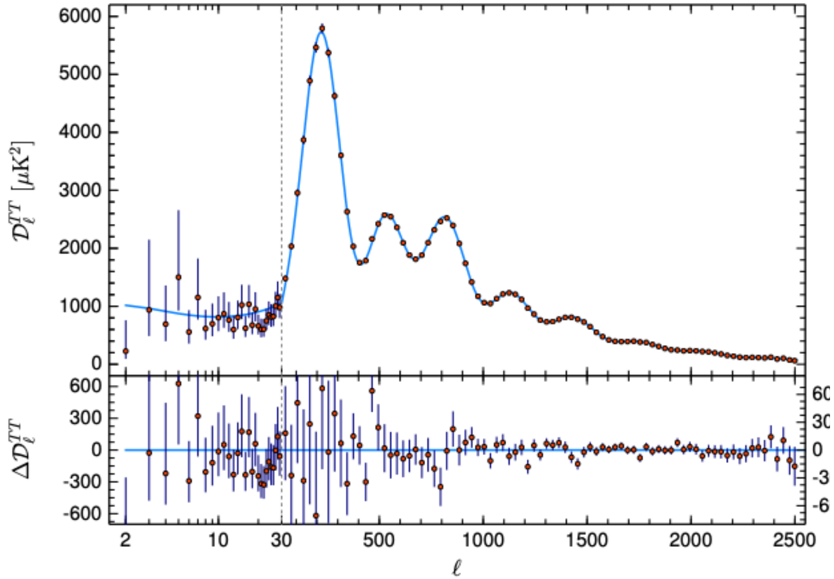

Fig. 1. *Planck* 2018 temperature power spectrum. At multipoles $\ell \geq 30$ we show the frequency-coadded temperature computed from the `Plik` cross-half-mission likelihood, with foreground and other nuisance parameters fixed to a best fit the base-ΛCDM cosmology. In the multipole range $2 \leq \ell \leq 29$, we plot the power spectrum estimates from the Co component-separation algorithm, computed over 86 % of the sky. The base-ΛCDM theoretical spectrum best fit to th TT,TE,EE+lowE+lensing likelihoods is plotted in light blue in the upper panel. Residuals with respect to this model are the lower panel. The error bars show $\pm 1\,\sigma$ diagonal uncertainties, including cosmic variance (approximated as Gaussian, including uncertainties in the foreground model at $\ell \geq 30$. Note that the vertical scale changes at $\ell = 30$, where the horizontal axis switches from logarithmic to linear.

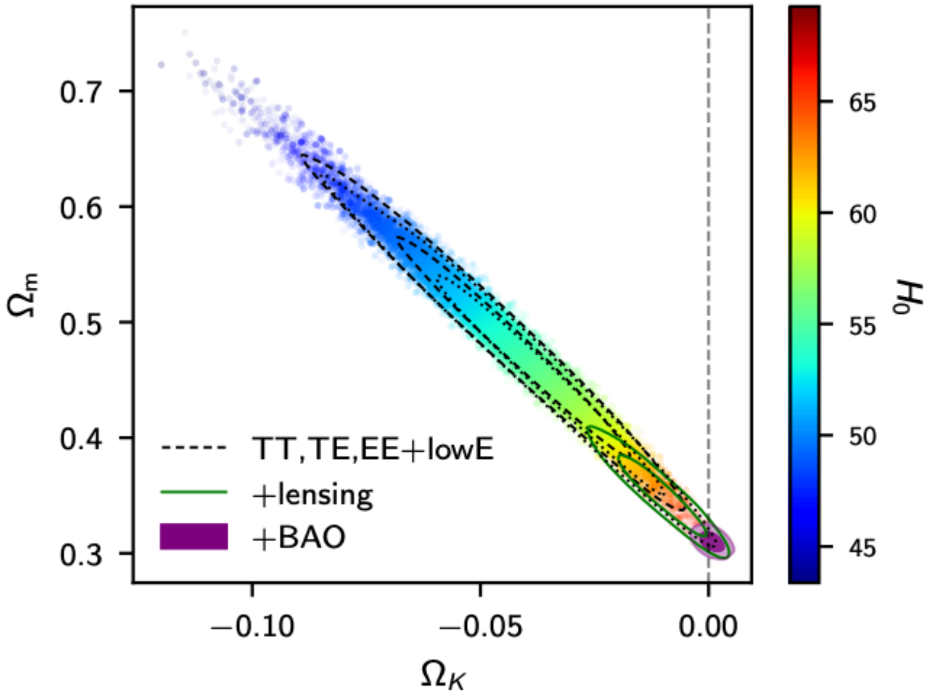

$|\Omega_K| \lesssim 0.1$

$R \approx 9000h^{-1}\mathrm{Mpc}$

Planck (2018)

Motivation

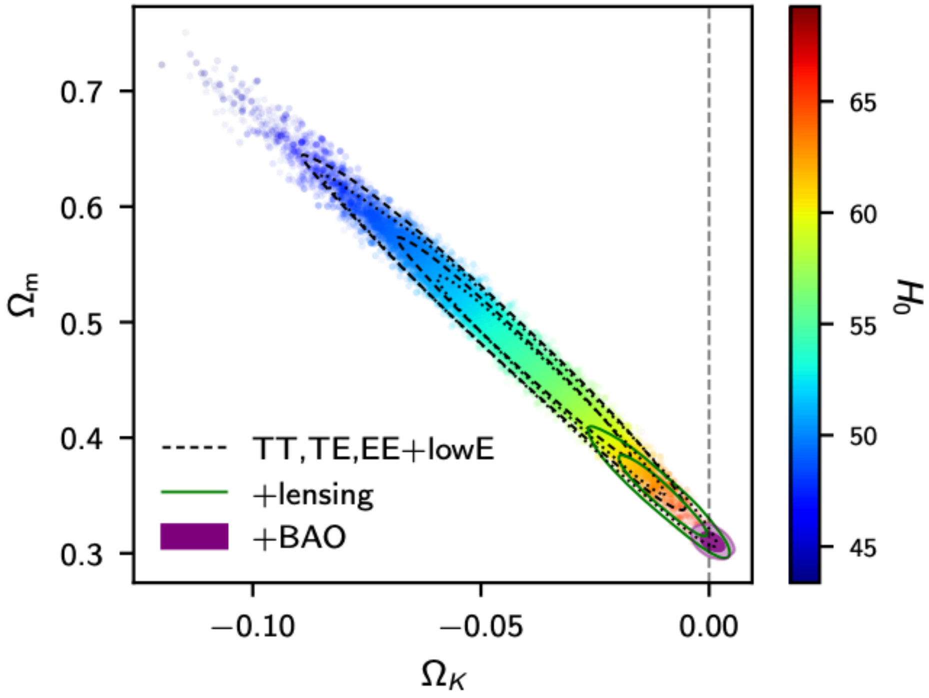

$|\Omega_K| \lesssim 0.1$

$R \approx 9000 h^{-1}\mathrm{Mpc}$

Planck (2018)

Euclid typical size:

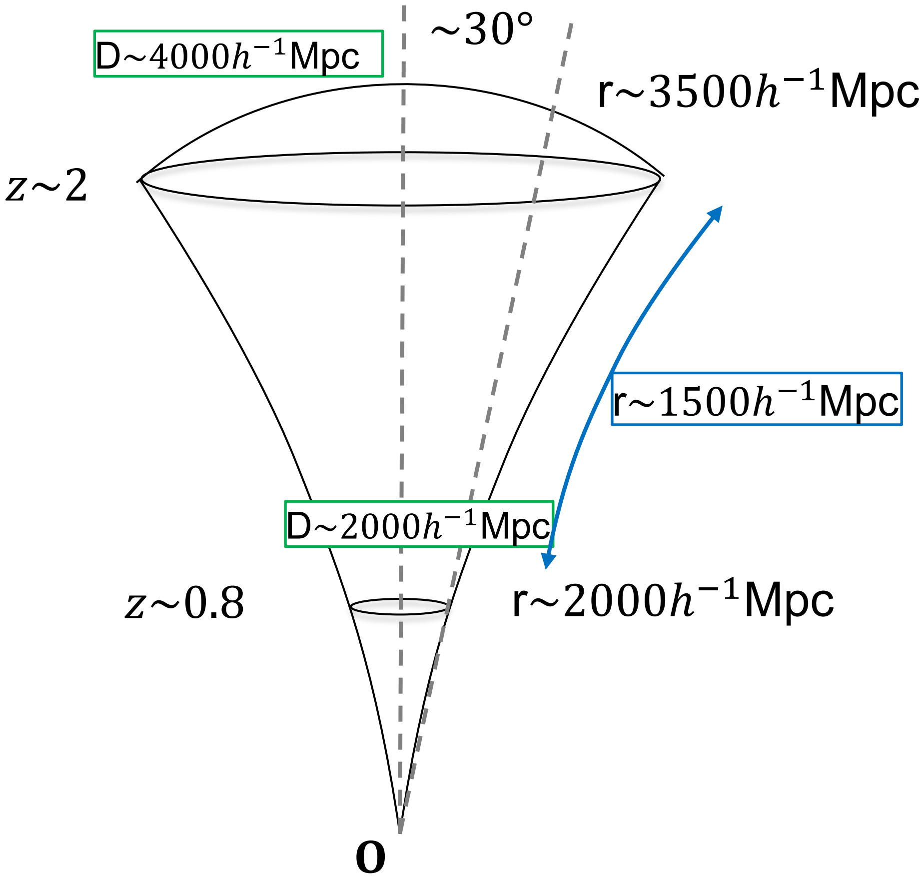

10 to 40 % of curvature scale

Formalism in curved space

Problem: Fourier basis in curved space ?

FLRW metric:

$$\mathrm{d}s^2 = c^2\,\mathrm{d}t^2 - a^2(t)\,\gamma_{ij}\,\mathrm{d}x^i\,\mathrm{d}x^j = c^2\,\mathrm{d}t^2 - a^2(t)\left[\mathrm{d}\chi^2 + S_K^2(\chi)\left(\mathrm{d}\theta^2 + \sin^2\theta\,\mathrm{d}\phi^2\right)\right]$$

The Fourier basis $\mathcal{Q}$ must be solution of the Helmholtz equation:

$$\tilde{\nabla}^2\mathcal{Q} = \frac{1}{\sqrt{\gamma}}\,\partial_i\left(\sqrt{\gamma}\,\gamma^{ij}\,\partial_j\,\mathcal{Q}\right) = -\tilde{k}^2\mathcal{Q}$$

where $\tilde{\nabla}^2 = a_0^2\,\nabla^2,\ \tilde{k} = a_0\,k$

$$\boxed{\mathcal{Q}(\chi,\theta,\phi) = R(\chi)Y_{lm}(\theta,\phi)}$$

Matsubara (2000)

Formalism in curved space

Problem: Fourier basis in curved space ?

FLRW metric:

$$\mathrm{d}s^2 = \boxed{c^2\,\mathrm{d}t^2} - a^2(t)\,\gamma_{ij}\,\mathrm{d}x^i\,\mathrm{d}x^j = c^2\,\mathrm{d}t^2 - a^2(t)\left[\mathrm{d}\chi^2 + S_K^2(\chi)\left(\mathrm{d}\theta^2 + \sin^2\theta\,\mathrm{d}\phi^2\right)\right]$$

Temporal part

The Fourier basis $\mathcal{Q}$ must be solution of the Helmholtz equation:

$$\tilde{\nabla}^2\mathcal{Q} = \frac{1}{\sqrt{\gamma}}\,\partial_i\left(\sqrt{\gamma}\,\gamma^{ij}\,\partial_j\,\mathcal{Q}\right) = -\tilde{k}^2\mathcal{Q}$$

where $\tilde{\nabla}^2 = a_0^2\,\nabla^2,\ \tilde{k} = a_0\,k$

$$\boxed{\mathcal{Q}(\chi,\theta,\phi) = R(\chi)Y_{lm}(\theta,\phi)}$$

Matsubara (2000)

Formalism in curved space

Problem: Fourier basis in curved space ?

FLRW metric:

$$\mathrm{d}s^2 = \boxed{c^2\,\mathrm{d}t^2} - \boxed{a^2(t)\,\gamma_{ij}\,\mathrm{d}x^i\,\mathrm{d}x^j} = c^2\,\mathrm{d}t^2 - a^2(t)\left[\mathrm{d}\chi^2 + S_K^2(\chi)\left(\mathrm{d}\theta^2 + \sin^2\theta\,\mathrm{d}\phi^2\right)\right]$$

Temporal part *Spatial part*

The Fourier basis $\mathcal{Q}$ must be solution of the Helmholtz equation:

$$\tilde{\nabla}^2\mathcal{Q} = \frac{1}{\sqrt{\gamma}}\,\partial_i\left(\sqrt{\gamma}\,\gamma^{ij}\,\partial_j\,\mathcal{Q}\right) = -\tilde{k}^2\mathcal{Q}$$

where $\tilde{\nabla}^2 = a_0^2\,\nabla^2,\ \tilde{k} = a_0\,k$

$$\boxed{\mathcal{Q}(\chi,\theta,\phi) = R(\chi)Y_{lm}(\theta,\phi)}$$

Matsubara (2000)

Formalism in curved space

Problem: Fourier basis in curved space ?

FLRW metric:

$$\mathrm{d}s^2 = \boxed{c^2\,\mathrm{d}t^2} - \boxed{a^2(t)\,\gamma_{ij}\,\mathrm{d}x^i\,\mathrm{d}x^j} = c^2\,\mathrm{d}t^2 - a^2(t)\left[\boxed{\mathrm{d}\chi^2} + S_K^2(\chi)\left(\mathrm{d}\theta^2 + \sin^2\theta\,\mathrm{d}\phi^2\right)\right]$$

Temporal part *Spatial part* *Radial part*

The Fourier basis $\mathcal{Q}$ must be solution of the Helmholtz equation:

$$\tilde{\nabla}^2\mathcal{Q} = \frac{1}{\sqrt{\gamma}}\partial_i\left(\sqrt{\gamma}\,\gamma^{ij}\,\partial_j\,\mathcal{Q}\right) = -\tilde{k}^2\mathcal{Q}$$

where $\tilde{\nabla}^2 = a_0^2\,\nabla^2,\ \tilde{k} = a_0\,k$

$$\boxed{\mathcal{Q}(\chi,\theta,\phi) = R(\chi)Y_{lm}(\theta,\phi)}$$

Matsubara (2000)

Formalism in curved space

Problem: Fourier basis in curved space ?

FLRW metric:

$$\mathrm{d}s^2 = c^2\,\mathrm{d}t^2 - a^2(t)\,\gamma_{ij}\,\mathrm{d}x^i\,\mathrm{d}x^j = c^2\,\mathrm{d}t^2 - a^2(t)\left[\mathrm{d}\chi^2 + S_K^2(\chi)\left(\mathrm{d}\theta^2 + \sin^2\theta\,\mathrm{d}\phi^2\right)\right]$$

Temporal part *Spatial part* *Radial part* *Angular part*

The Fourier basis $\mathcal{Q}$ must be solution of the Helmholtz equation:

$$\tilde{\nabla}^2\mathcal{Q} = \frac{1}{\sqrt{\gamma}}\,\partial_i\left(\sqrt{\gamma}\,\gamma^{ij}\,\partial_j\,\mathcal{Q}\right) = -\tilde{k}^2\mathcal{Q}$$

where $\tilde{\nabla}^2 = a_0^2\,\nabla^2,\ \tilde{k} = a_0\,k$

$$\mathcal{Q}(\chi,\theta,\phi) = R(\chi)Y_{lm}(\theta,\phi)$$

Matsubara (2000)

Formalism in curved space

Problem: Fourier basis in curved space ?

FLRW metric:

$$\mathrm{d}s^2 = c^2\,\mathrm{d}t^2 - a^2(t)\,\gamma_{ij}\,\mathrm{d}x^i\,\mathrm{d}x^j = c^2\,\mathrm{d}t^2 - a^2(t)\left[\mathrm{d}\chi^2 + S_K^2(\chi)\left(\mathrm{d}\theta^2 + \sin^2\theta\,\mathrm{d}\phi^2\right)\right]$$

Temporal part *Spatial part* *Radial part* *Angular part*

The Fourier basis $\mathcal{Q}$ must be solution of the Helmholtz equation:

$$\tilde{\nabla}^2\mathcal{Q} = \frac{1}{\sqrt{\gamma}}\partial_i\left(\sqrt{\gamma}\,\gamma^{ij}\,\partial_j\,\mathcal{Q}\right) = -\tilde{k}^2\mathcal{Q}$$

where $\tilde{\nabla}^2 = a_0^2\,\nabla^2, \;\tilde{k} = a_0\,k$

$$\mathcal{Q}(\chi,\theta,\phi) = R(\chi)Y_{lm}(\theta,\phi)$$

Spherical Harmonics

Galaxy clustering in configuration space

Redshift space distortions on linear scale:

$$\delta_{\mathrm{g}}^{s}(z,\boldsymbol{r}) = b(z)\delta_{\mathrm{m}}(z,\boldsymbol{r}) - \frac{(1+z)}{H(z)}\frac{\partial}{\partial r}\left[\boldsymbol{v}(z,\boldsymbol{r})\cdot\hat{\boldsymbol{r}}\right] - \frac{(1+z)}{H(z)}\alpha(z)\left[\boldsymbol{v}(z,\boldsymbol{r})\cdot\hat{\boldsymbol{r}}\right] + \left[5s(z)-2\right]\kappa(z,\boldsymbol{r}) + \delta_{\Phi}(z,\boldsymbol{r})$$

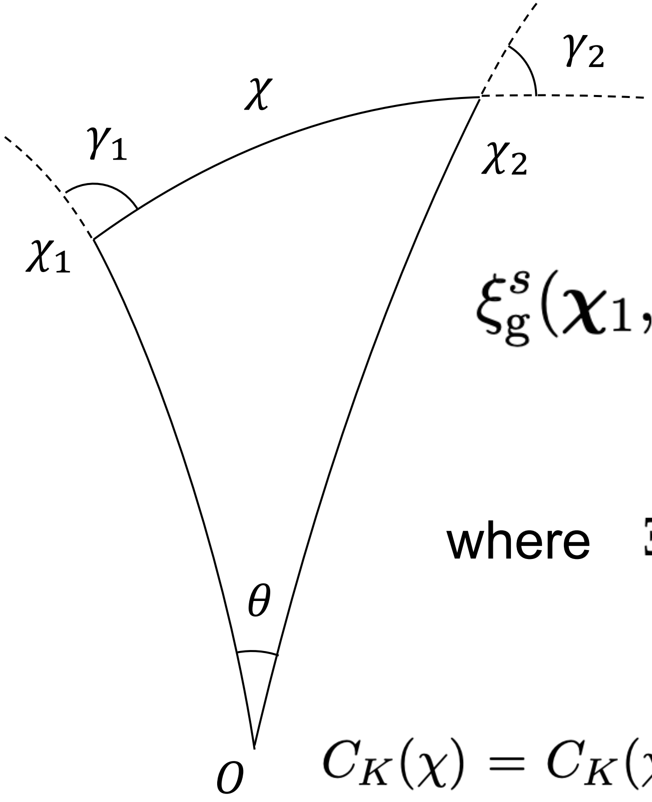

Matsubara (2000)

$$\xi_{\mathrm{g}}^{s}(\boldsymbol{\chi}_1,\boldsymbol{\chi}_2) = b_1 b_2 D_1 D_2 \sum_{n,l} c_l^{(n)}(\chi_1,\chi_2,\theta)\,\Xi_l^{(n)}(\chi)$$

where $\Xi_l^{(n)}(\chi) = 4\pi(-1)^n \int \mathrm{d}\nu\, \frac{\nu^2}{(\nu^2-4K)^n}\mathcal{S}(\nu)X_l^{(K)}(\nu,\chi)$

$$C_K(\chi) = C_K(\chi_1)C_K(\chi_2) + K\,S_K(\chi_1)S_K(\chi_2)\cos\theta$$

Galaxy clustering in configuration space

Redshift space distortions on linear scale:

$$\delta^s_{\rm g}(z,\boldsymbol{r}) = \boxed{b(z)\delta_{\rm m}(z,\boldsymbol{r})} - \frac{(1+z)}{H(z)}\frac{\partial}{\partial r}\left[\boldsymbol{v}(z,\boldsymbol{r})\cdot\hat{\boldsymbol{r}}\right] - \frac{(1+z)}{H(z)}\alpha(z)\left[\boldsymbol{v}(z,\boldsymbol{r})\cdot\hat{\boldsymbol{r}}\right] + \left[5s(z)-2\right]\kappa(z,\boldsymbol{r}) + \delta_\Phi(z,\boldsymbol{r})$$

Linear bias

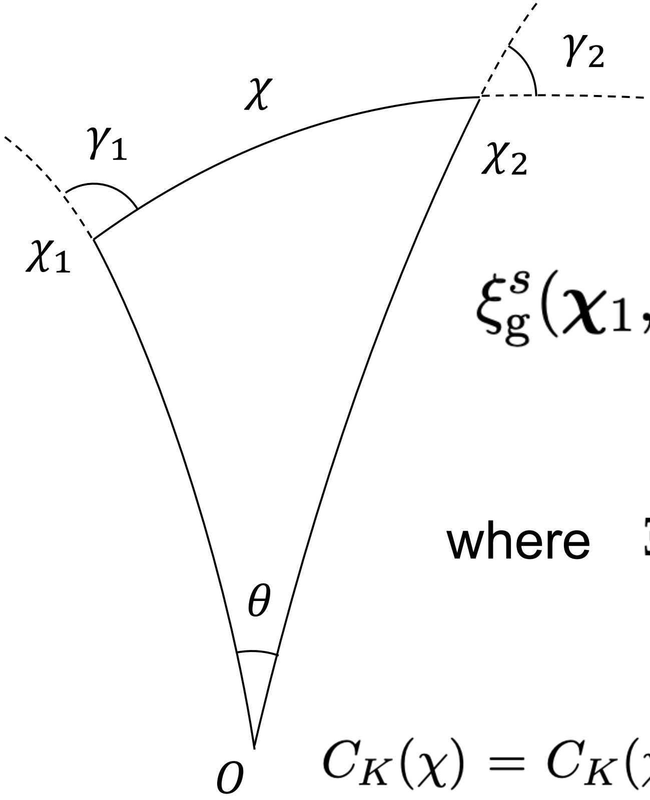

Matsubara (2000)

$$\xi^s_{\rm g}(\boldsymbol{\chi}_1,\boldsymbol{\chi}_2) = b_1 b_2 D_1 D_2 \sum_{n,l} c_l^{(n)}(\chi_1,\chi_2,\theta)\,\Xi_l^{(n)}(\chi)$$

where $\Xi_l^{(n)}(\chi) = 4\pi(-1)^n \int \mathrm{d}\nu\, \frac{\nu^2}{(\nu^2-4K)^n}\mathcal{S}(\nu)X_l^{(K)}(\nu,\chi)$

$$C_K(\chi) = C_K(\chi_1)C_K(\chi_2) + K\, S_K(\chi_1)S_K(\chi_2)\cos\theta$$

Galaxy clustering in configuration space

Redshift space distortions on linear scale:

Peculiar velocity term

$$\delta^s_{\mathrm{g}}(z,\boldsymbol{r}) = \boxed{b(z)\delta_{\mathrm{m}}(z,\boldsymbol{r})} - \boxed{\frac{(1+z)}{H(z)}\frac{\partial}{\partial r}\left[\boldsymbol{v}(z,\boldsymbol{r})\cdot\hat{\boldsymbol{r}}\right]}$$

Linear bias

$$-\frac{(1+z)}{H(z)}\alpha(z)\left[\boldsymbol{v}(z,\boldsymbol{r})\cdot\hat{\boldsymbol{r}}\right] + \left[5s(z)-2\right]\kappa(z,\boldsymbol{r}) + \delta_\Phi(z,\boldsymbol{r})$$

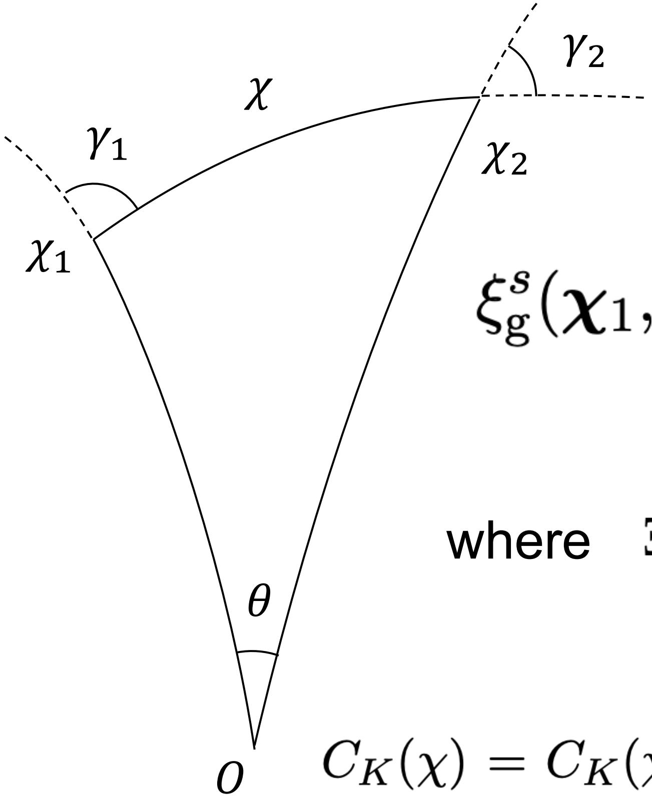

Matsubara (2000)

$$\xi^s_{\mathrm{g}}(\boldsymbol{\chi}_1,\boldsymbol{\chi}_2) = b_1 b_2 D_1 D_2 \sum_{n,l} c_l^{(n)}(\chi_1,\chi_2,\theta)\,\Xi_l^{(n)}(\chi)$$

where $\Xi_l^{(n)}(\chi) = 4\pi(-1)^n \int \mathrm{d}\nu\, \frac{\nu^2}{(\nu^2-4K)^n}\mathcal{S}(\nu)X_l^{(K)}(\nu,\chi)$

$$C_K(\chi) = C_K(\chi_1)C_K(\chi_2) + K\, S_K(\chi_1)S_K(\chi_2)\cos\theta$$

Galaxy clustering in configuration space

Redshift space distortions on linear scale:

Peculiar velocity term

$$\delta_{\rm g}^{s}(z,\boldsymbol{r}) = b(z)\delta_{\rm m}(z,\boldsymbol{r}) - \frac{(1+z)}{H(z)}\frac{\partial}{\partial r}\left[\boldsymbol{v}(z,\boldsymbol{r})\cdot\hat{\boldsymbol{r}}\right] - \frac{(1+z)}{H(z)}\alpha(z)\left[\boldsymbol{v}(z,\boldsymbol{r})\cdot\hat{\boldsymbol{r}}\right] + \left[5s(z)-2\right]\kappa(z,\boldsymbol{r}) + \delta_{\Phi}(z,\boldsymbol{r})$$

Linear bias

Relativistic effects

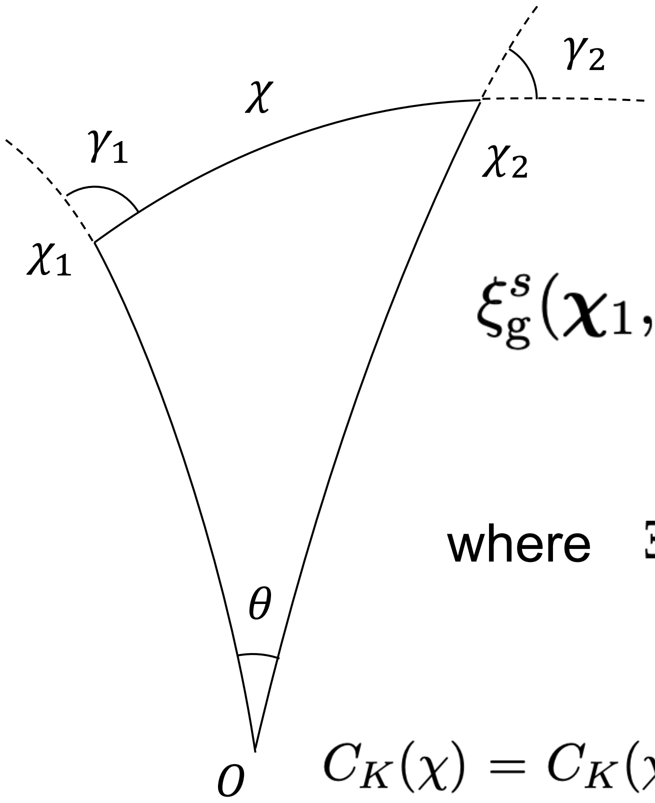

Matsubara (2000)

$$\xi_{\rm g}^{s}(\boldsymbol{\chi}_1,\boldsymbol{\chi}_2) = b_1 b_2 D_1 D_2 \sum_{n,l} c_l^{(n)}(\chi_1,\chi_2,\theta)\,\Xi_l^{(n)}(\chi)$$

where $\Xi_l^{(n)}(\chi) = 4\pi(-1)^n \int {\rm d}\nu\, \frac{\nu^2}{(\nu^2-4K)^n}\mathcal{S}(\nu)X_l^{(K)}(\nu,\chi)$

$$C_K(\chi) = C_K(\chi_1)C_K(\chi_2) + K\,S_K(\chi_1)S_K(\chi_2)\cos\theta$$

Results

We use galaxy clustering data publicly available:

Clustering ratio (CR)

$$\eta_R(r) \equiv \frac{\xi_R^{(0)}(r)}{\sigma_R^2}$$

- No bias
- No RSD
- No redshift evolution

It probes the shape of the power spectrum

Data set		$z_{\rm min}$	$z_{\rm max}$	η_R	Ref.
SDSS	DR7	0.15	0.43	0.096 ± 0.007	[44, 61]
	DR12	0.30	0.53	0.094 ± 0.006	[44, 62]
	DR12	0.53	0.67	0.105 ± 0.011	[44, 62]

Bel & Marinoni (2014)
Zennaro et al. (2018)

$f\sigma_8$ parameter (RSD)

It probes the matter velocity field through anisotropy of the galaxy clustering induced by redshift space distortions

Data set	z	$f\sigma_8$	Reference
2MTF	0.001	0.505 ± 0.085	[28]
6dFGS+SNIa	0.02	0.428 ± 0.0465	[29]
IRAS+SNIa	0.02	0.398 ± 0.065	[30, 31]
2MASS	0.02	0.314 ± 0.048	[31, 32]
SDSS	0.10	0.376 ± 0.038	[33]
SDSS-MGS	0.15	0.490 ± 0.145	[34]
2dFGRS	0.17	0.510 ± 0.060	[35]
GAMA	0.18	0.360 ± 0.090	[36]
GAMA	0.38	0.440 ± 0.060	[36]
SDSS-LRG-200	0.25	0.3512 ± 0.0583	[37]
SDSS-LRG-200	0.37	0.4602 ± 0.0378	[37]
BOSS DR12	0.31	0.469 ± 0.098	[38]
BOSS DR12	0.36	0.474 ± 0.097	[38]
BOSS DR12	0.40	0.473 ± 0.086	[38]
BOSS DR12	0.44	0.481 ± 0.076	[38]
BOSS DR12	0.48	0.482 ± 0.067	[38]
BOSS DR12	0.52	0.488 ± 0.065	[38]
BOSS DR12	0.56	0.482 ± 0.067	[38]
BOSS DR12	0.59	0.481 ± 0.066	[38]
BOSS DR12	0.64	0.486 ± 0.070	[38]
WiggleZ	0.44	0.413 ± 0.080	[39]
WiggleZ	0.60	0.390 ± 0.063	[39]
WiggleZ	0.73	0.437 ± 0.072	[39]
Vipers PDR-2	0.60	0.550 ± 0.120	[40, 41]
Vipers PDR-2	0.86	0.400 ± 0.110	[40, 41]
FastSound	1.40	0.482 ± 0.116	[42]
SDSS-IV	0.978	0.379 ± 0.176	[43]
SDSS-IV	1.23	0.385 ± 0.099	[43]
SDSS-IV	1.526	0.342 ± 0.070	[43]
SDSS-IV	1.944	0.364 ± 0.106	[43]

-> Alcock-Paczynski

Results

Cosmological constraints on KLCDM models:

Parameter	Prior
$\Omega_{\mathrm{b},0}h^2$	$[0,\ 100]$
$\Omega_{\mathrm{c},0}h^2$	$[0,\ 100]$
H_0	$[40,\ 100]$
τ	$[0,\ 0.2]$
$\ln(10^{10}A_\mathrm{s})$	$[0,\ 100]$
n_s	$[0.9,\ 1]$
$\Omega_{K,0}$	$[-0.2,\ 0.6]$
$\Omega_{\mathrm{b},0}h^2$	$\mathcal{N}\left(0.0222, 0.0005^2\right)$
$\sigma_{8,0}$	$[0.6,\ 1]$
$\Omega_{\mathrm{m},0}$	$[0,\ 1]$

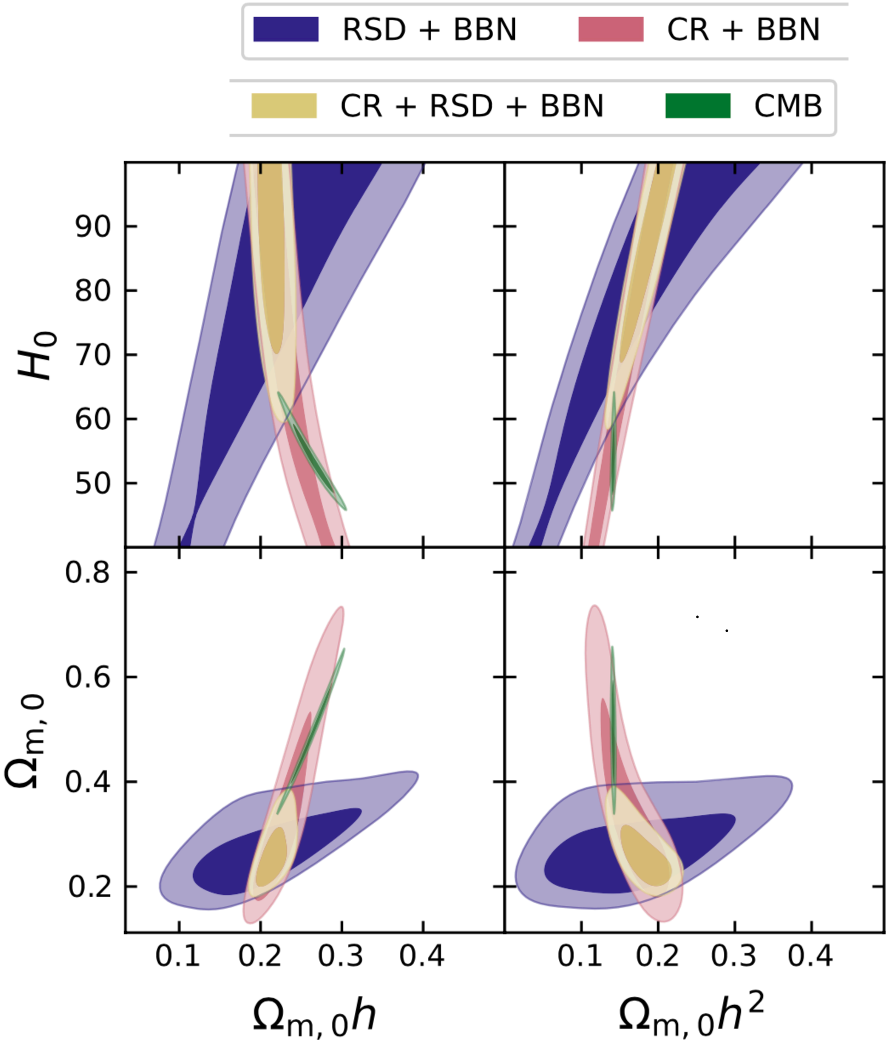

Results

Cosmological constraints on KLCDM models:

Parameter	Prior
$\Omega_{b,0}h^2$	[0, 100]
$\Omega_{c,0}h^2$	[0, 100]
H_0	[40, 100]
τ	[0, 0.2]
$\ln(10^{10}A_s)$	[0, 100]
n_s	[0.9, 1]
$\Omega_{K,0}$	[−0.2, 0.6]
$\Omega_{b,0}h^2$	$\mathcal{N}(0.0222, 0.0005^2)$
$\sigma_{8,0}$	[0.6, 1]
$\Omega_{m,0}$	[0, 1]

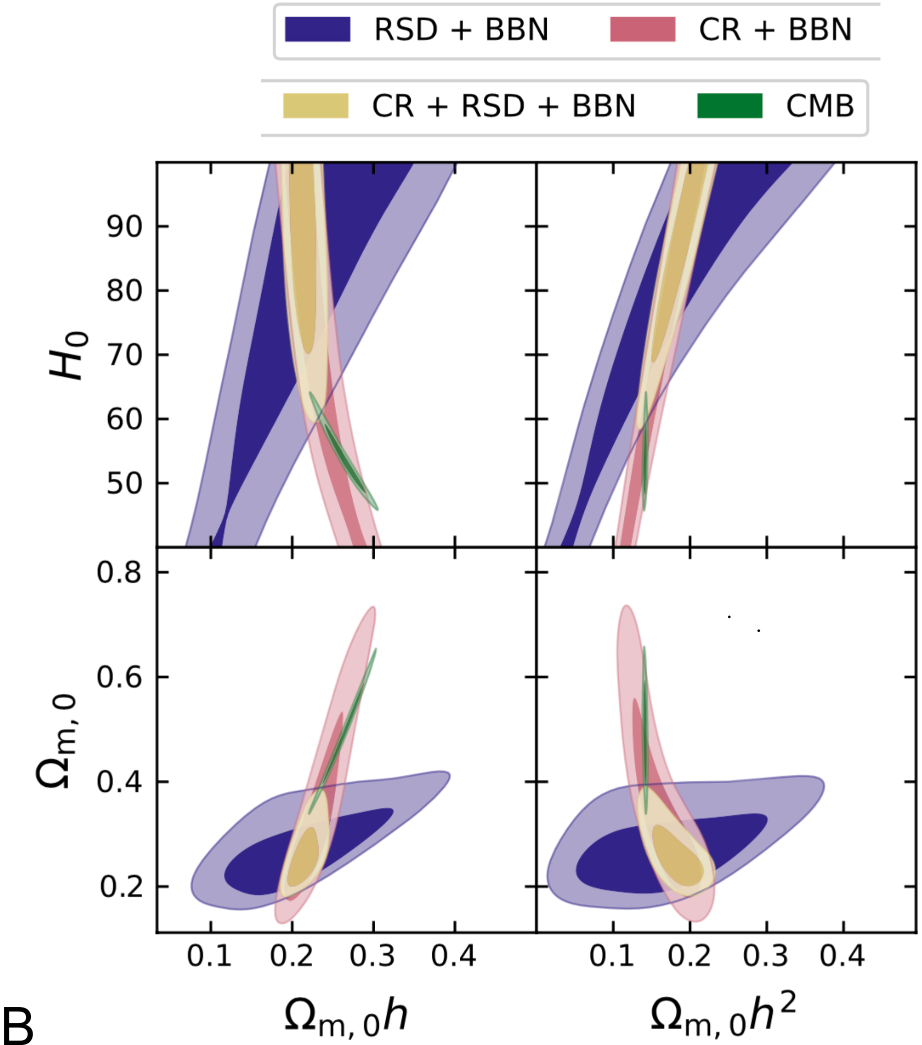

H_0 (> 62 km/s/Mpc at 95% C.L.)

-> completely independent from CMB

Results

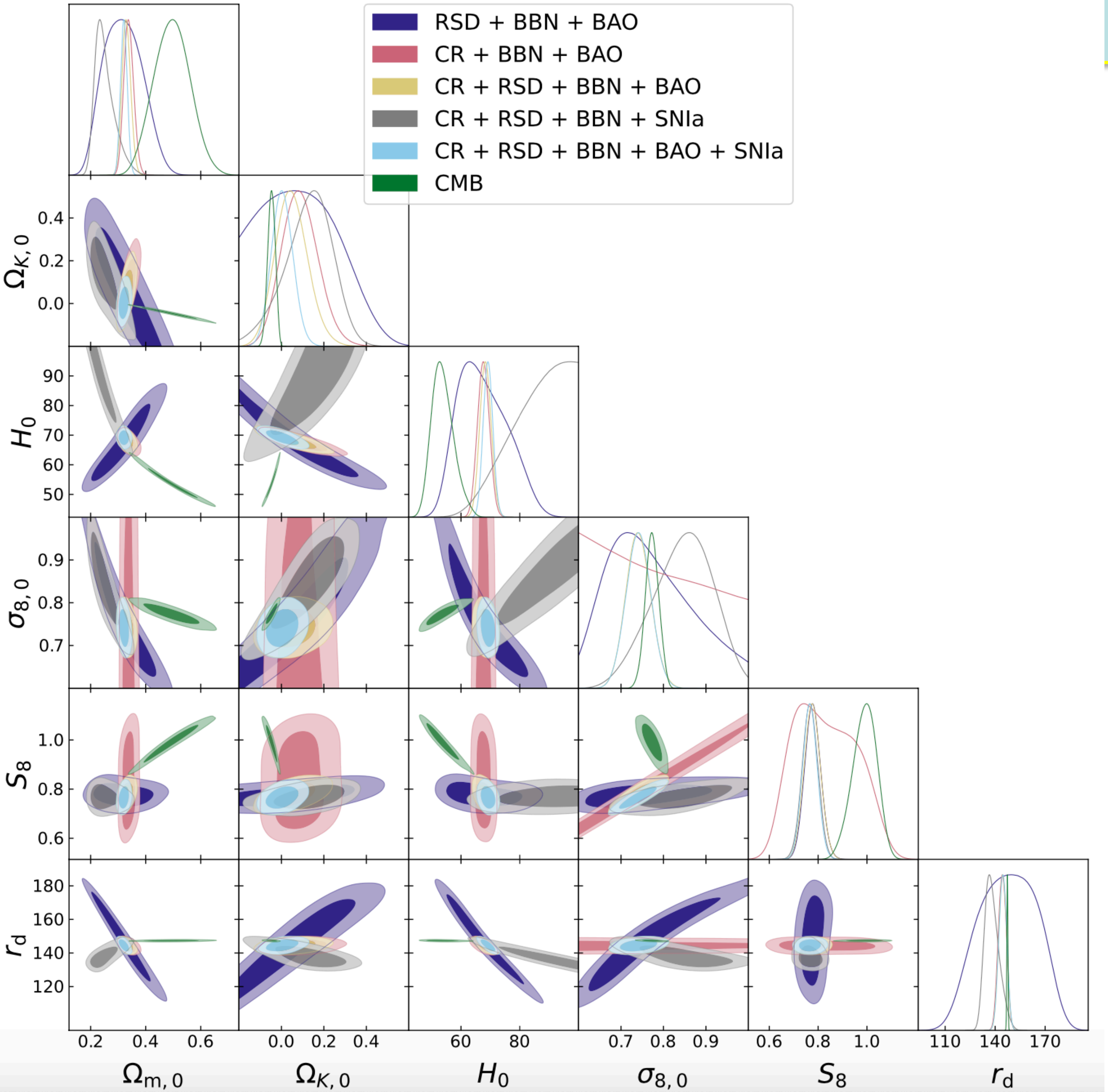
RSD + BBN + BAO
CR + BBN + BAO
CR + RSD + BBN + BAO
CR + RSD + BBN + SNIa
CR + RSD + BBN + BAO + SNIa
CMB
$\Omega_{K,0}$
0.4
0.2
0.0
H_0
90
80
70
60
50
$\sigma_{8,0}$
0.9
0.8
0.7
S_8
1.0
0.8
0.6
r_d
180
160
140
120
0.2 0.4 0.6
$\Omega_{\mathrm{m},0}$
0.0 0.2 0.4
$\Omega_{K,0}$
60 80
H_0
0.7 0.8 0.9
$\sigma_{8,0}$
0.6 0.8 1.0
S_8
110 140 170
r_d

Results

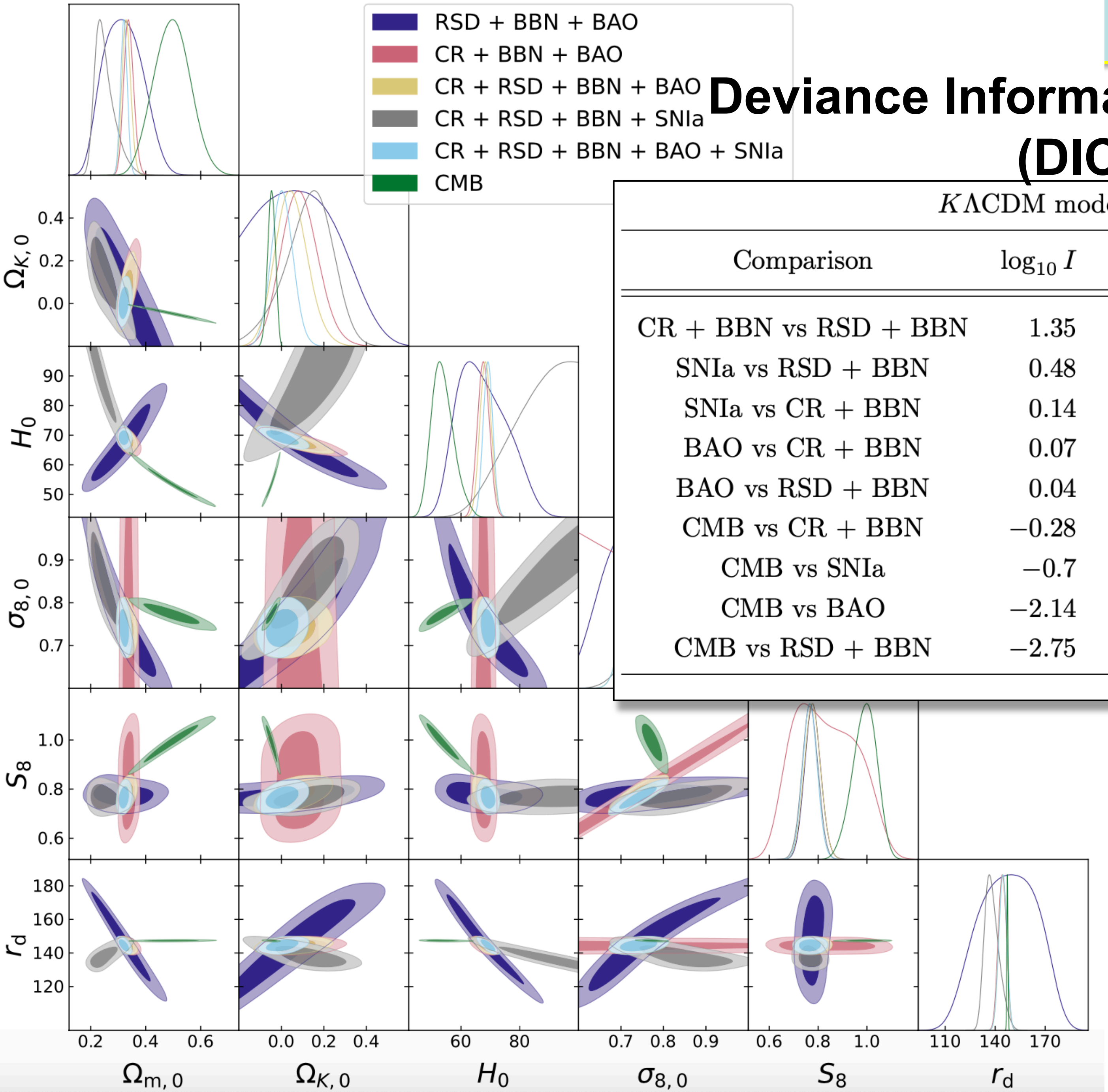

Deviance Information Criterion (DIC)

$K\Lambda$CDM model

Comparison	$\log_{10} I$	Agreement / Disagreement
CR + BBN vs RSD + BBN	1.35	strong agreement
SNIa vs RSD + BBN	0.48	inconclusive
SNIa vs CR + BBN	0.14	inconclusive
BAO vs CR + BBN	0.07	inconclusive
BAO vs RSD + BBN	0.04	inconclusive
CMB vs CR + BBN	−0.28	inconclusive
CMB vs SNIa	−0.7	substantial
CMB vs BAO	−2.14	decisive disagreement
CMB vs RSD + BBN	−2.75	decisive disagreement

Results

Deviance Information Criterion (DIC)

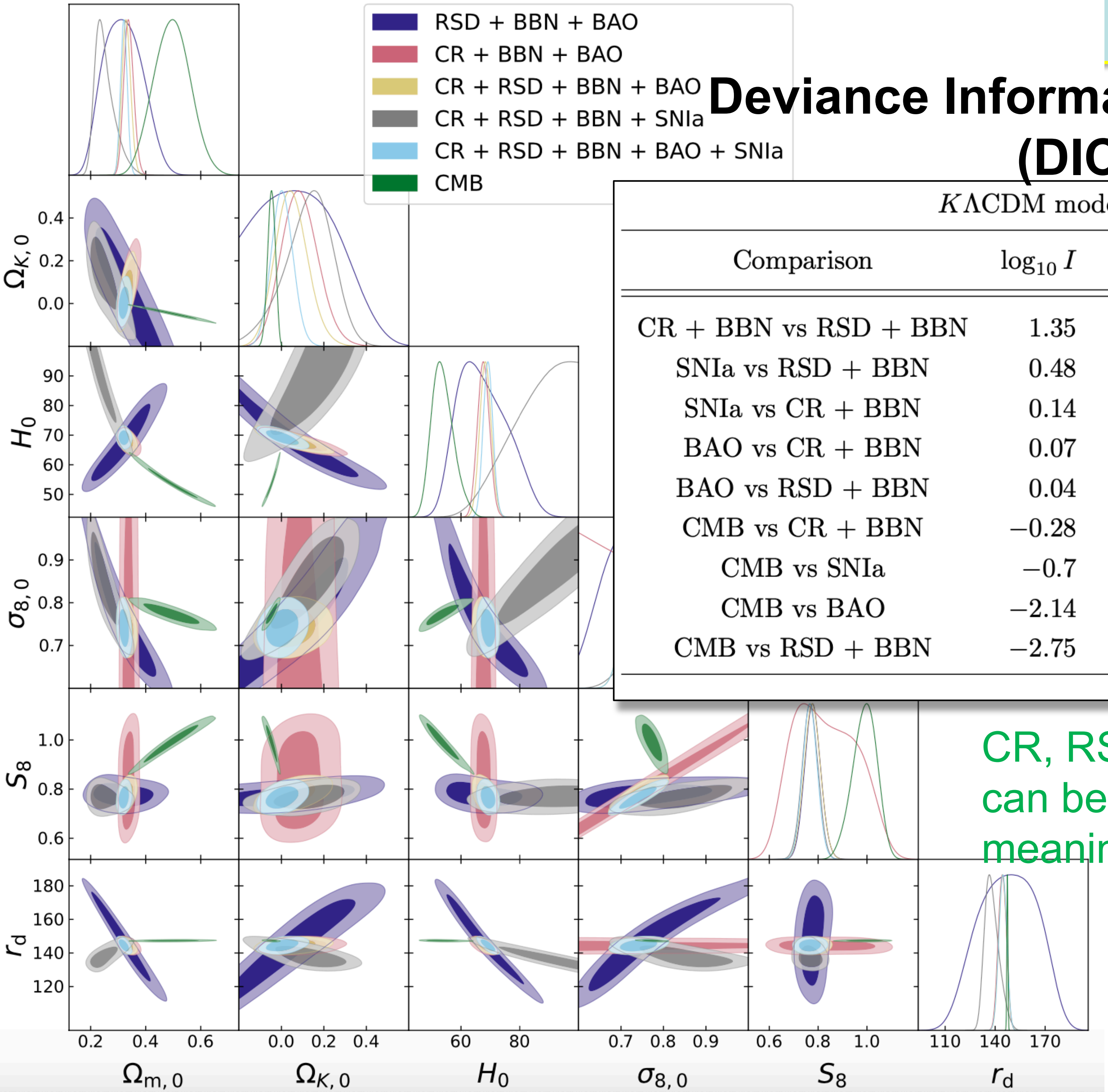

$K\Lambda$CDM model

Comparison	$\log_{10} I$	Agreement / Disagreement
CR + BBN vs RSD + BBN	1.35	strong agreement
SNIa vs RSD + BBN	0.48	inconclusive
SNIa vs CR + BBN	0.14	inconclusive
BAO vs CR + BBN	0.07	inconclusive
BAO vs RSD + BBN	0.04	inconclusive
CMB vs CR + BBN	−0.28	inconclusive
CMB vs SNIa	−0.7	substantial
CMB vs BAO	−2.14	decisive disagreement
CMB vs RSD + BBN	−2.75	decisive disagreement

CR, RSD, BAO and SNIa can be combined in a meaningful way

Results

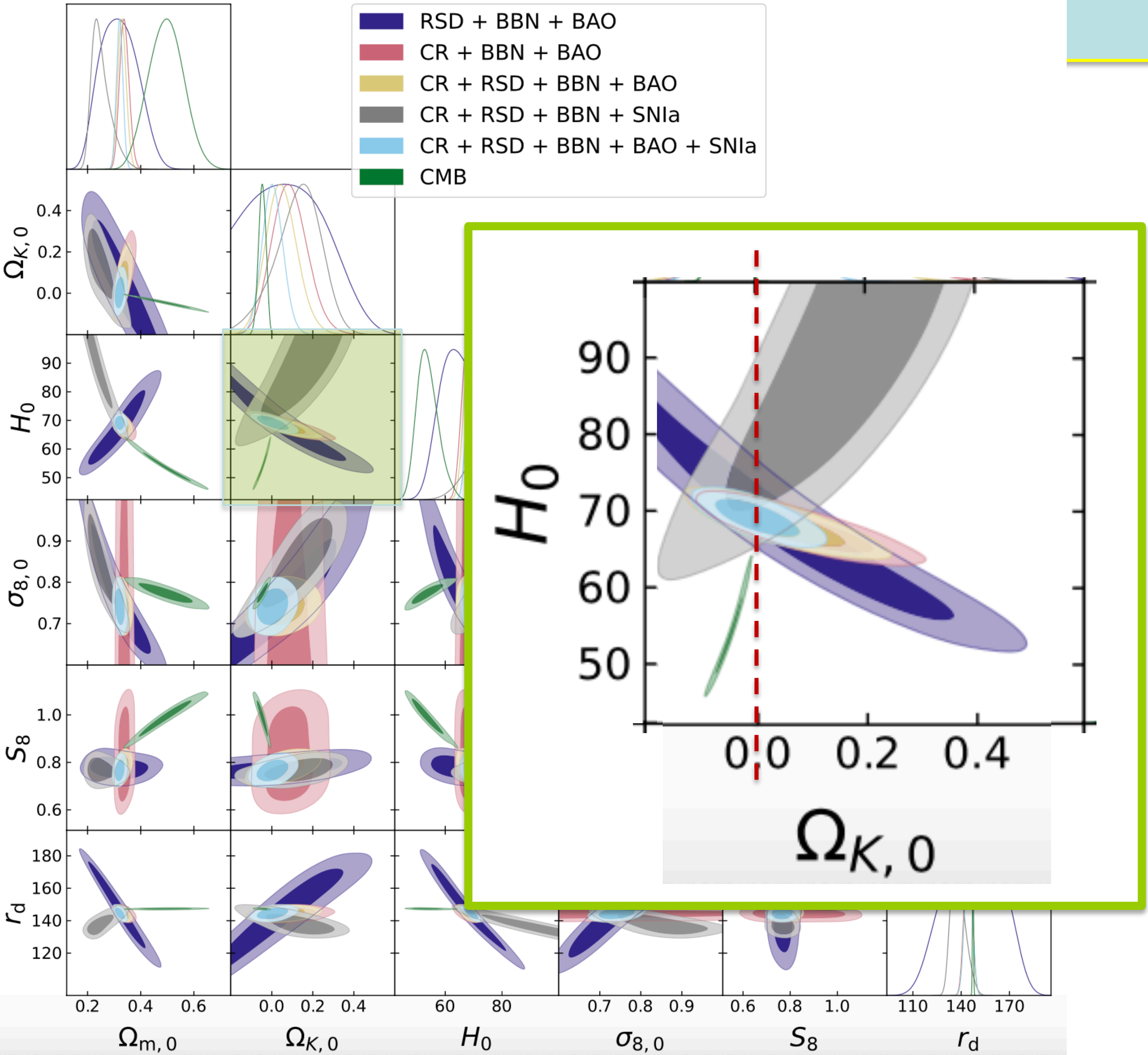
RSD + BBN + BAO
CR + BBN + BAO
CR + RSD + BBN + BAO
CR + RSD + BBN + SNIa
CR + RSD + BBN + BAO + SNIa
CMB
$\Omega_{K,0}$
0.4
0.2
0.0
H_0
90
80
70
60
50
$\sigma_{8,0}$
0.9
0.8
0.7
S_8
1.0
0.8
0.6
r_d
180
160
140
120
0.2
0.4
0.6
$\Omega_{\mathrm{m},0}$
0.0
0.2
0.4
$\Omega_{K,0}$
60
80
H_0
0.7
0.8
0.9
$\sigma_{8,0}$
0.6
0.8
1.0
S_8
110
140
170
r_d
90
80
70
60
50
H_0
0.0
0.2
0.4
$\Omega_{K,0}$

Results

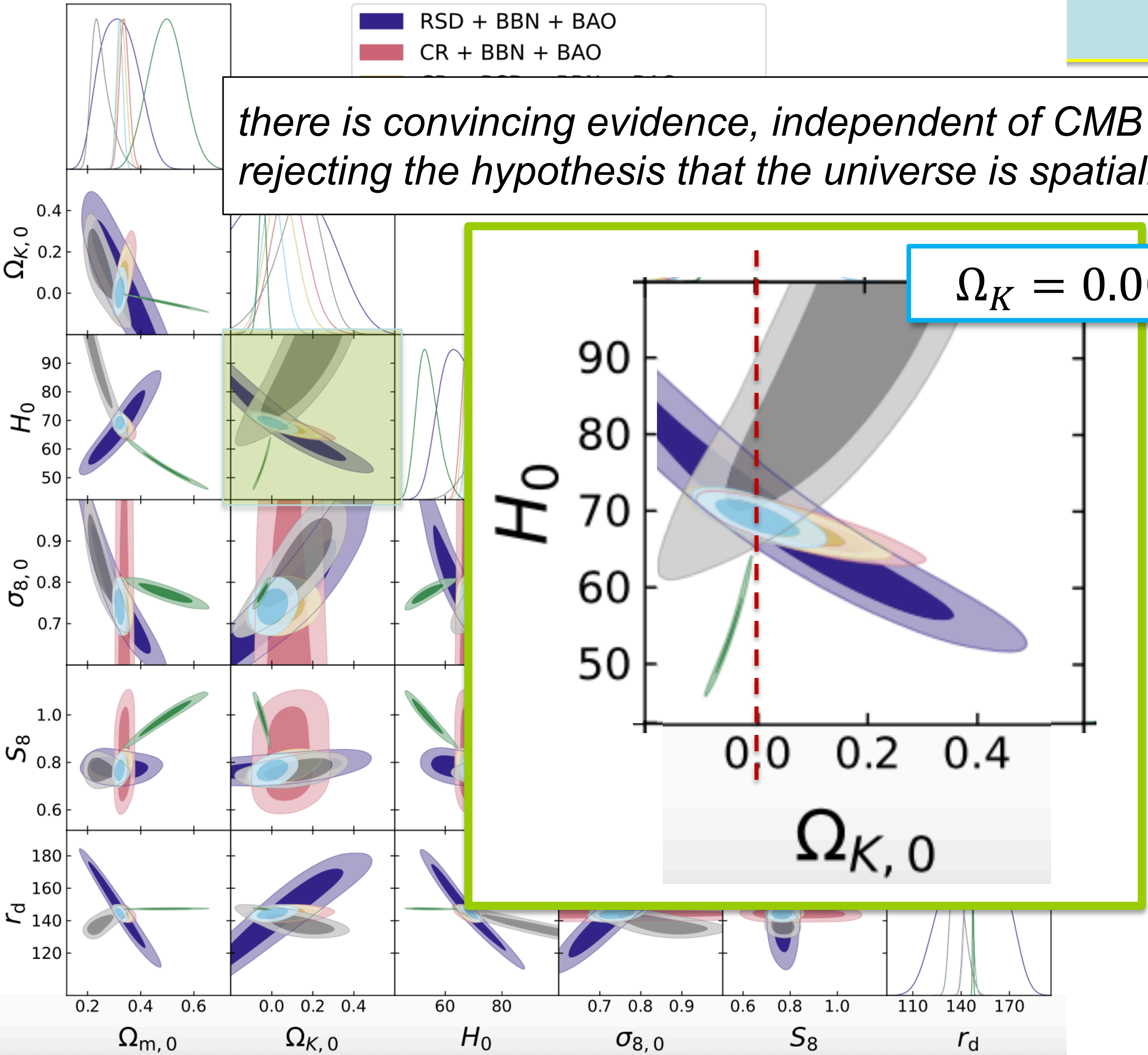

there is convincing evidence, independent of CMB data, for not rejecting the hypothesis that the universe is spatially flat

$$\Omega_K = 0.004 \pm 0.05$$

Results

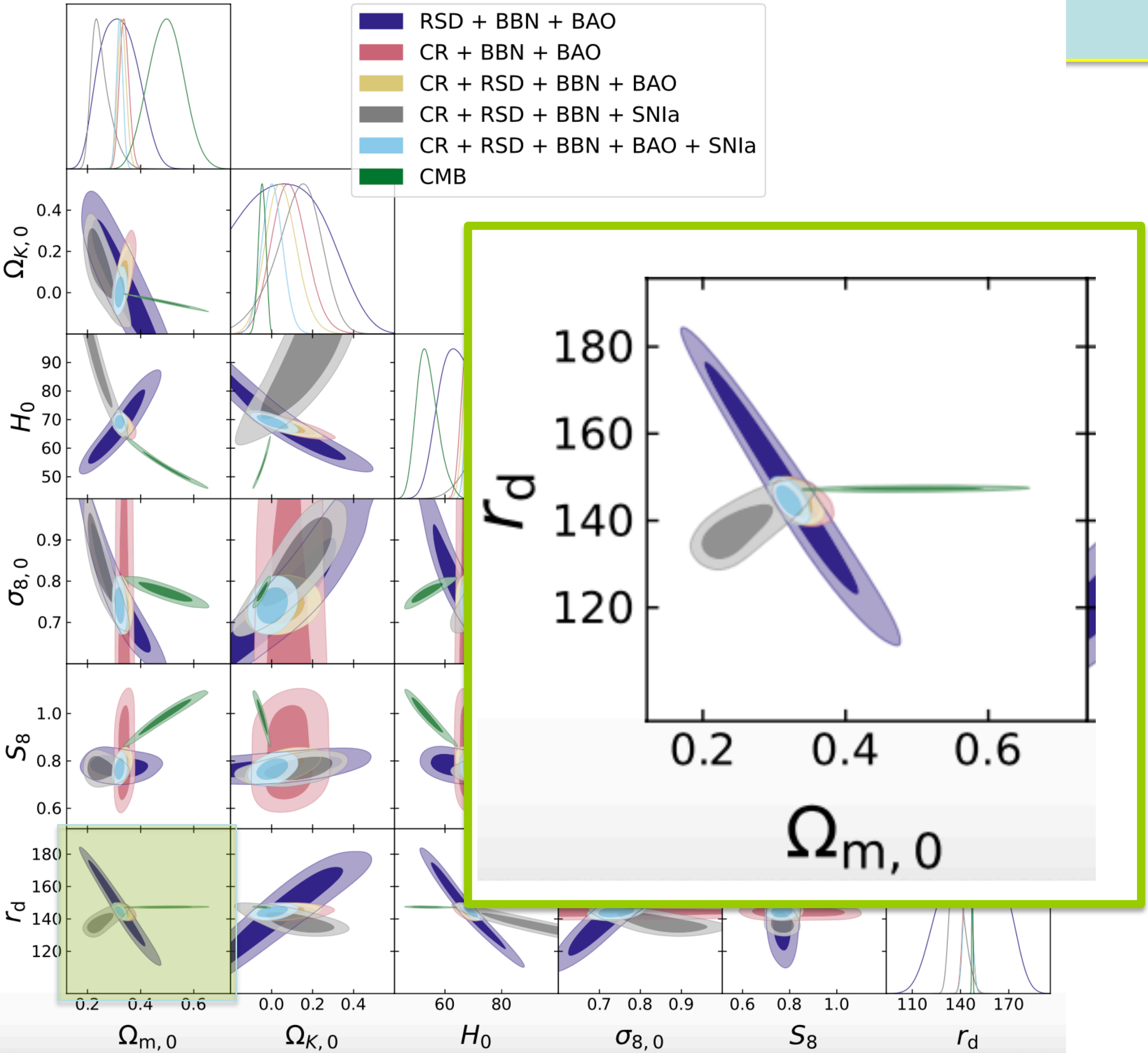
RSD + BBN + BAO
CR + BBN + BAO
CR + RSD + BBN + BAO
CR + RSD + BBN + SNIa
CR + RSD + BBN + BAO + SNIa
CMB
$\Omega_{K,0}$
0.4
0.2
0.0
H_0
90
80
70
60
50
$\sigma_{8,0}$
0.9
0.8
0.7
S_8
1.0
0.8
0.6
r_d
180
160
140
120
0.2 0.4 0.6
$\Omega_{m,0}$
0.0 0.2 0.4
$\Omega_{K,0}$
60 80
H_0
0.7 0.8 0.9
$\sigma_{8,0}$
0.6 0.8 1.0
S_8
110 140 170
r_d
180
160
140
120
r_d
0.2
0.4
0.6
$\Omega_{m,0}$

Results

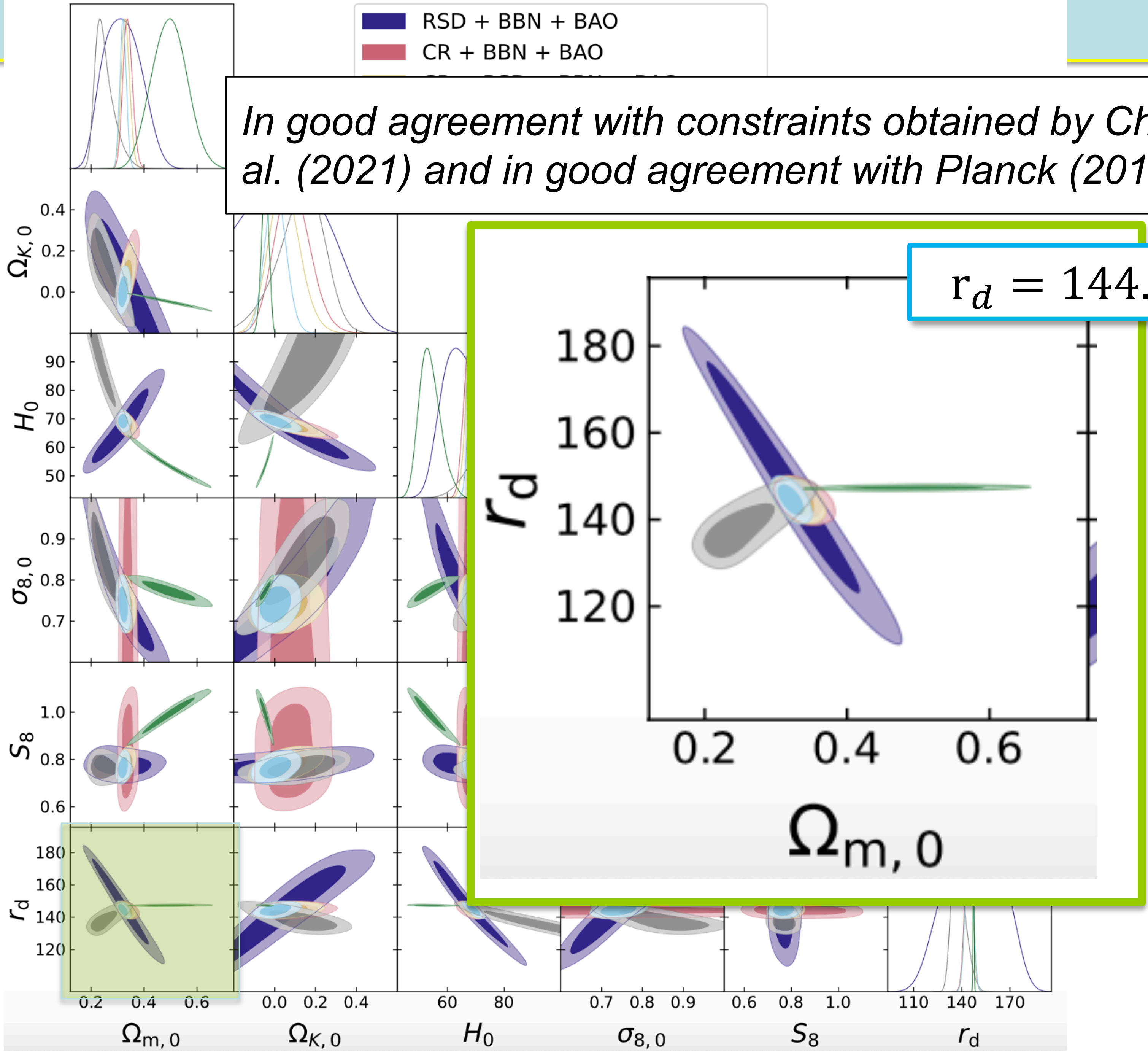

In good agreement with constraints obtained by Chudaykin et al. (2021) and in good agreement with Planck (2018)

$r_d = 144.57 \pm 2.34$

(Mpc)

Results

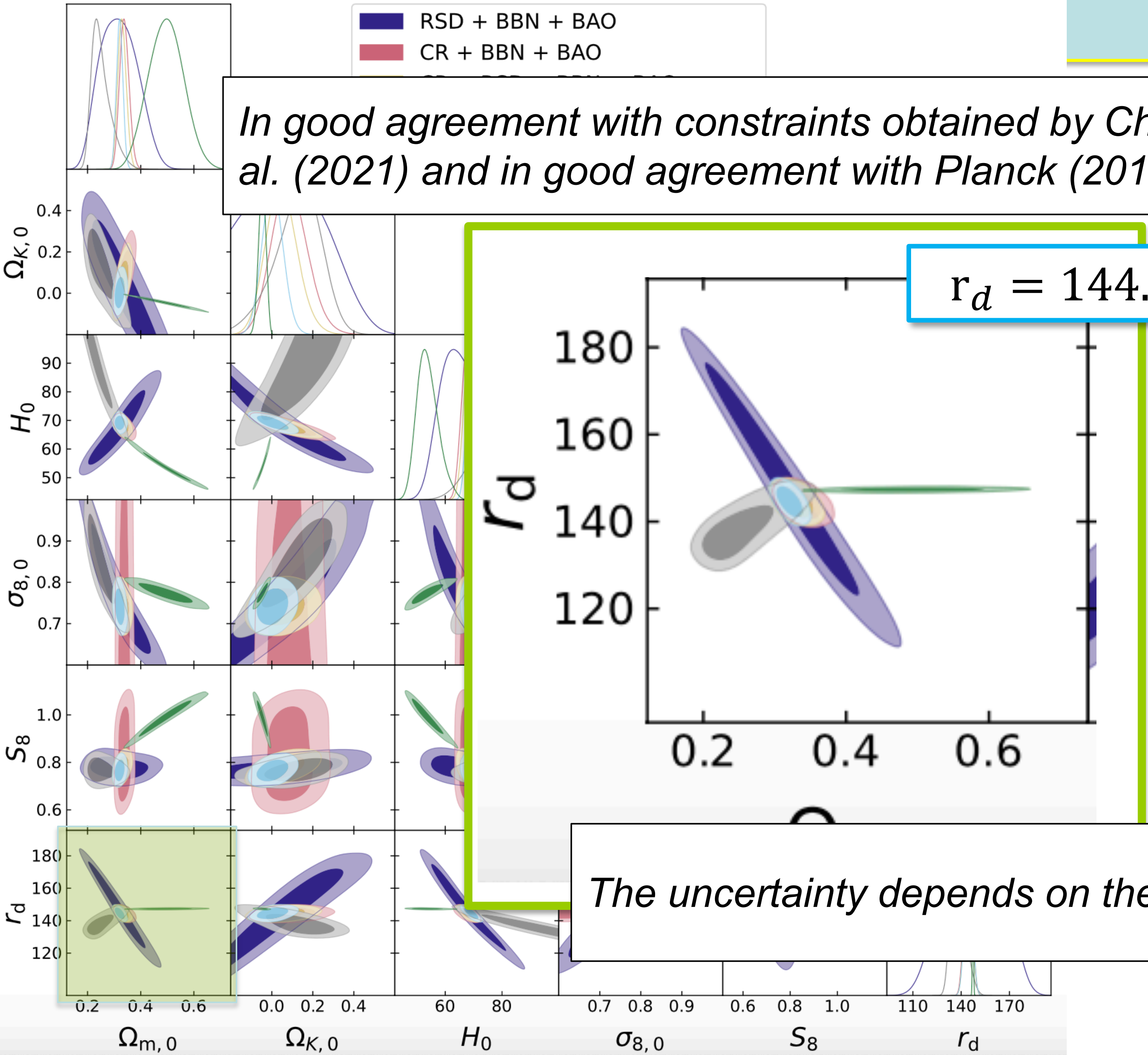

In good agreement with constraints obtained by Chudaykin et al. (2021) and in good agreement with Planck (2018)

$r_d = 144.57 \pm 2.34$

(Mpc)

The uncertainty depends on the BBN prior

Results

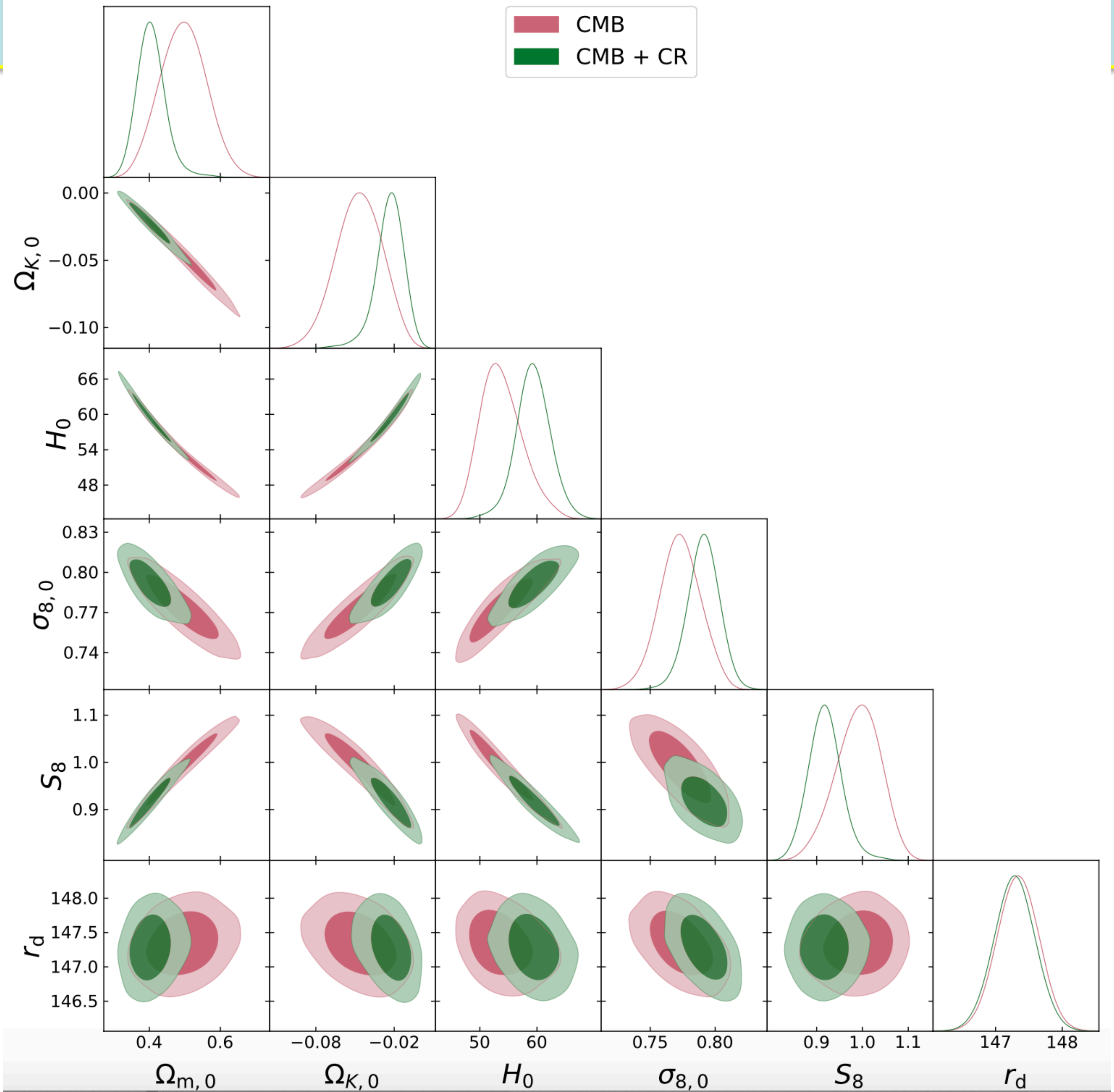
CMB
CMB + CR
$\Omega_{K,0}$
0.00
−0.05
−0.10
H_0
66
60
54
48
$\sigma_{8,0}$
0.83
0.80
0.77
0.74
S_8
1.1
1.0
0.9
r_d
148.0
147.5
147.0
146.5
0.4
0.6
$\Omega_{m,0}$
−0.08
−0.02
$\Omega_{K,0}$
50
60
H_0
0.75
0.80
$\sigma_{8,0}$
0.9
1.0
1.1
S_8
147
148
r_d

Results

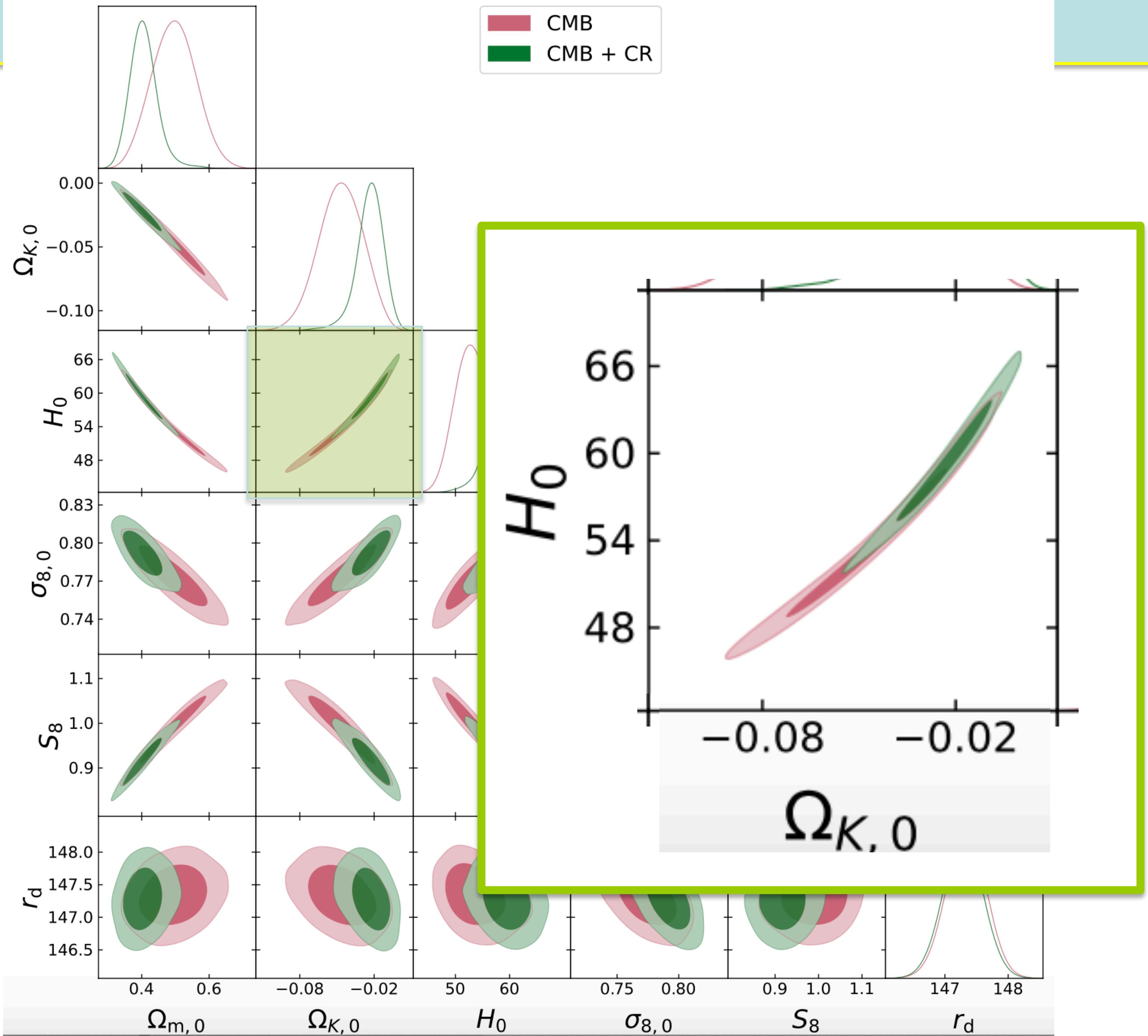
CMB
CMB + CR
0.00
−0.05
−0.10
$\Omega_{K,0}$
66
60
54
48
H_0
0.83
0.80
0.77
0.74
$\sigma_{8,0}$
1.1
1.0
0.9
S_8
148.0
147.5
147.0
146.5
$r_{\rm d}$
0.4
0.6
$\Omega_{\rm m,0}$
−0.08
−0.02
$\Omega_{K,0}$
50
60
H_0
0.75
0.80
$\sigma_{8,0}$
0.9
1.0
1.1
S_8
147
148
$r_{\rm d}$
66
60
54
48
H_0
−0.08
−0.02
$\Omega_{K,0}$

Results

The flat LCDM model cannot be rejected, there is a too high risk of rejecting the wrong model

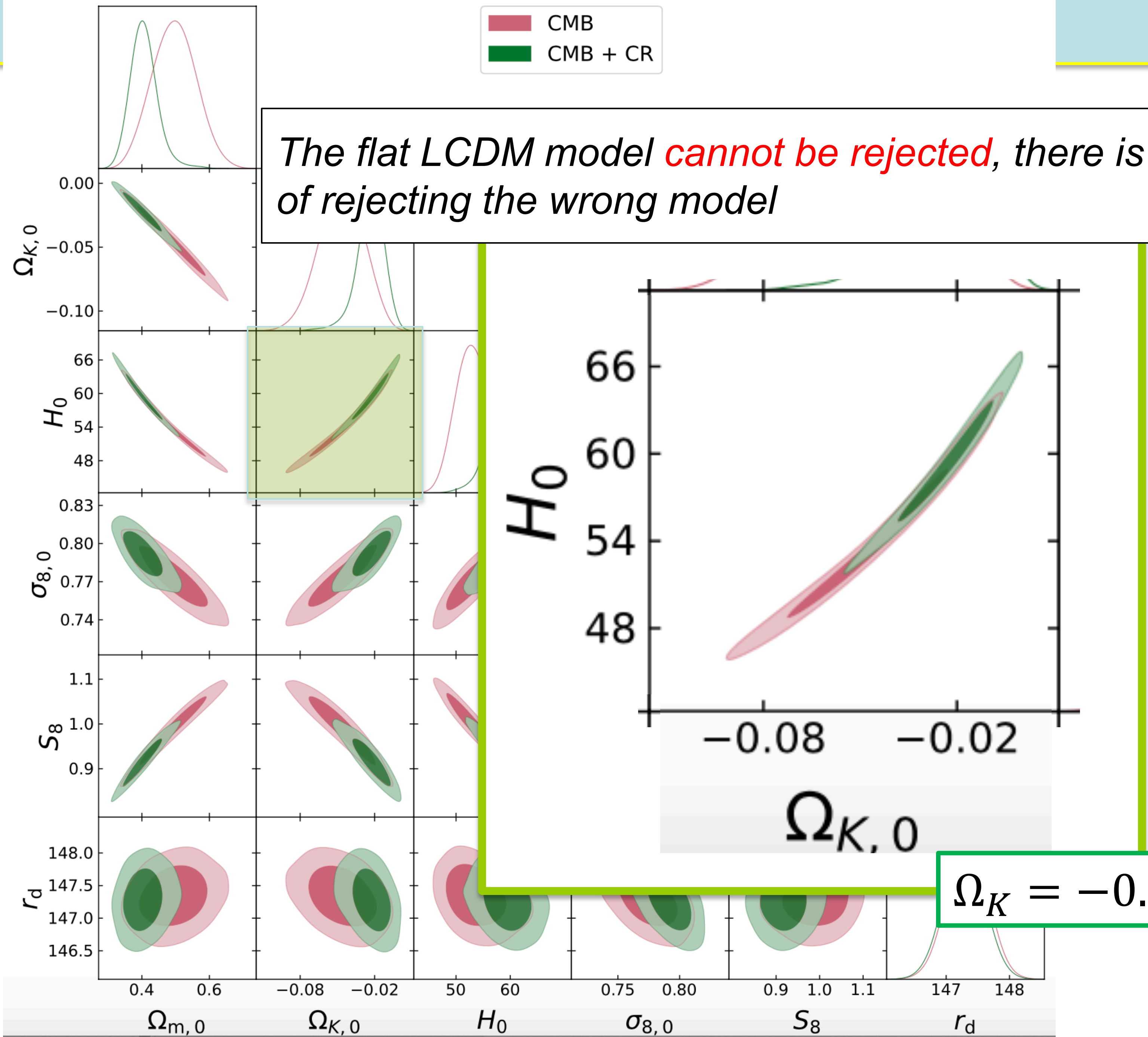

$$\Omega_K = -0.023 \pm 0.01$$

Conclusion

-Clustering alone (CR+RSD+BBN) allows to set a lower bound on H_0 (> 62 km/s/Mpc at 95% C.L.)

-CR+RSD+BBN+BAO+SNIa allow to constrain curvature $\Omega_K = 0.004 \pm 0.05$

-According to DIC statistics the CR data do not disagree with CMB contrary to RSD and BAO it provides $\Omega_K = -0.023 \pm 0.01$ (cannot reject flatLCDM)

- CR+RSD+BBN+BAO+SNIa sound horizon $r_d = 144.57 \pm 2.34\ \mathrm{Mpc}$ compatible with CMB

Formalism in curved space

Statistical invariance: cross-correlation between Fourier modes:

$$\left\langle \delta_{lm}(\nu)\delta^*_{l'm'}(\nu')\right\rangle = \delta_{ll'}\,\delta_{mm'}\,\frac{\mathcal{S}(\nu)}{\nu^2}\begin{cases}\delta^{\mathrm{D}}(\nu-\nu') & \text{if} \quad K \leq 0, \\ \delta_{\nu\nu'} & \text{if} \quad K = 1.\end{cases}$$

-> There is no cross-correlation, only the power spectrum $\underline{\mathcal{S}(\nu)}$

$$\nu\,\mathcal{S}(\nu) = \frac{k}{a_0^2}\,P(k) \quad \text{where} \quad k = \frac{\tilde{k}}{a_0} = \frac{\sqrt{\nu^2 - K}}{a_0} \quad \text{and} \quad \tilde{k}\,\chi = k\,r.$$

Formalism in curved space

Power spectrum:

$\underline{\mathcal{S}(\nu)}$

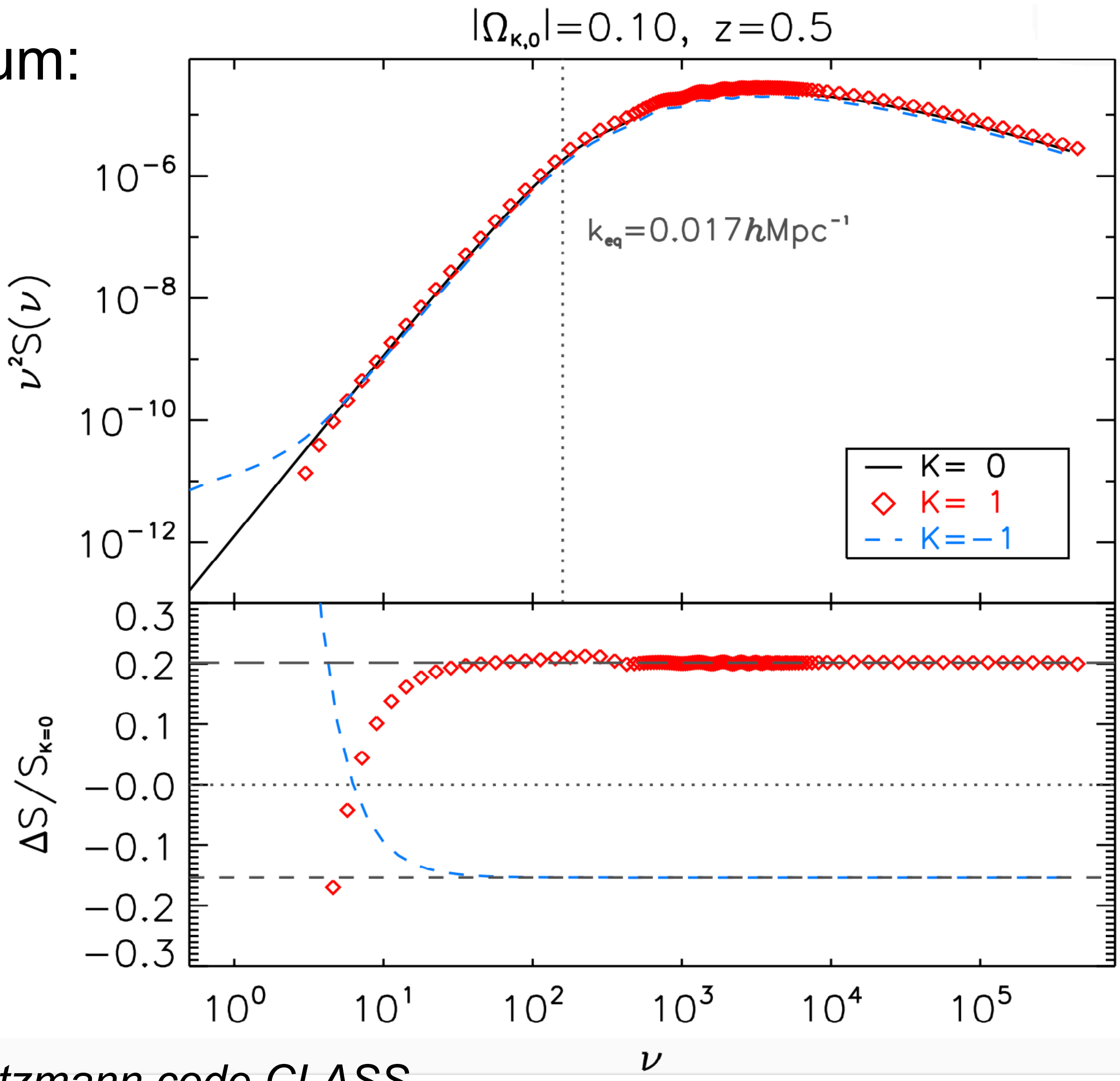

Output from the Boltzmann code CLASS

Formalism in curved space

The matter, galaxy or halo density contrast can be expanded on the Fourier basis:

$$\delta(\chi,\theta,\phi) = 4\pi \int_0^\infty \mathrm{d}\nu\, \nu^2 \sum_{l=0}^{\infty} \sum_{m=-l}^{l} \delta_{lm}(\nu)\, \hat{X}_l^{(K)}(\nu,\chi)\, Y_{lm}(\theta,\phi),$$

where $\hat{X}_l^{(K)}(\nu,\chi)$ is the radial part of the Fourier basis and for convenience one can define the effective wave number ν as

$$\tilde{k}^2 = \nu^2 - K$$

The Fourier transform of the density contrast can be expressed

$$\delta_{lm}(\nu) = \frac{1}{2\pi^2} \int \mathrm{d}^2\Omega\, \mathrm{d}\chi\, S_K^2(\chi)\, \delta(\chi,\theta,\phi) \hat{X}_l^{(K)}(\nu,\chi) Y_{lm}^*(\theta,\phi)$$

Galaxy clustering in configuration space

Multipole expansion of the 2-point correlation function:

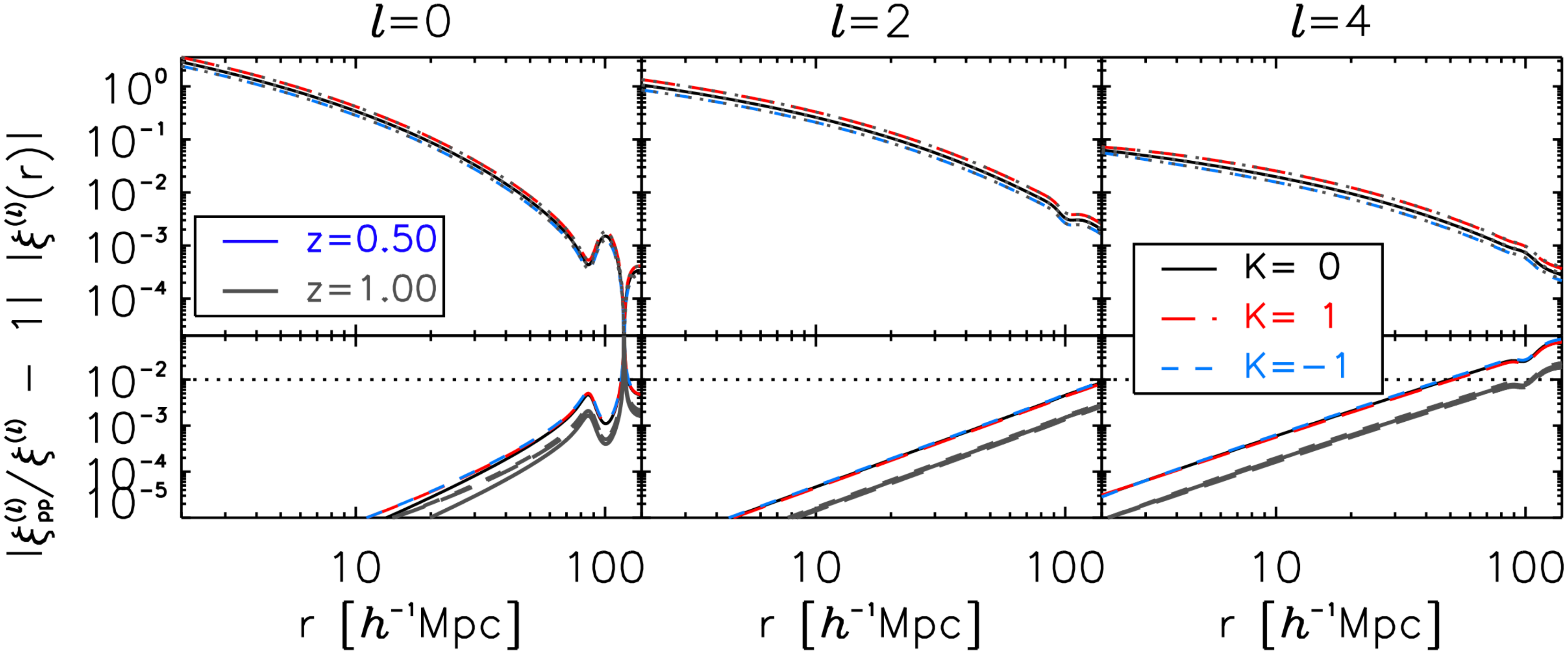

The hexadecapol is the most affected by **wide angle effects**

Deviance Information Criterion (DIC)

Be D1 and D2 to data set, are those two data set in tension ?

$DIC(D) = 2\overline{\chi^2_{eff}} - \chi^2_{eff}$ where $\chi^2_{eff} = -2\ln\mathcal{L}_{max}$

$\mathcal{L}_{max}$ is the maximum likelihood

$\overline{\chi^2_{eff}}$ average over the posterior

$$I(D_1, D_2) = \mathrm{e}^{-\mathcal{F}(D_1,D_2)/2} \quad \text{where } \mathcal{F}(D_1, D_2) = \mathrm{DIC}(D_1 \cup D_2) - \mathrm{DIC}(D_1) - \mathrm{DIC}(D_2)$$

If $\log_{10} I > 0$ there is agreement else there is disagreement

Jeffrey scale:

$\lvert\log_{10} I\rvert > 0.5$	-> *substantial*
$\lvert\log_{10} I\rvert > 1.0$	-> *strong*
$\lvert\log_{10} I\rvert > 2.0$	-> *decisive*

Alcock-Paczynski

2-point correlation function density of pairs of object

$$\tilde{\xi}^s_{\rm g}(\tilde{r}, \tilde{\mu}) = \xi^s_{\rm g}(r, \mu)$$

where

$$r = \tilde{r}\, \alpha_\perp \left[1 + \left(\lambda^2 - 1\right) \tilde{\mu}^2\right]^{1/2}, \qquad \mu = \tilde{\mu}\, \lambda \left[1 + \left(\lambda^2 - 1\right) \tilde{\mu}^2\right]^{-1/2} \quad \text{where } \lambda = \frac{\alpha_\parallel}{\alpha_\perp}.$$

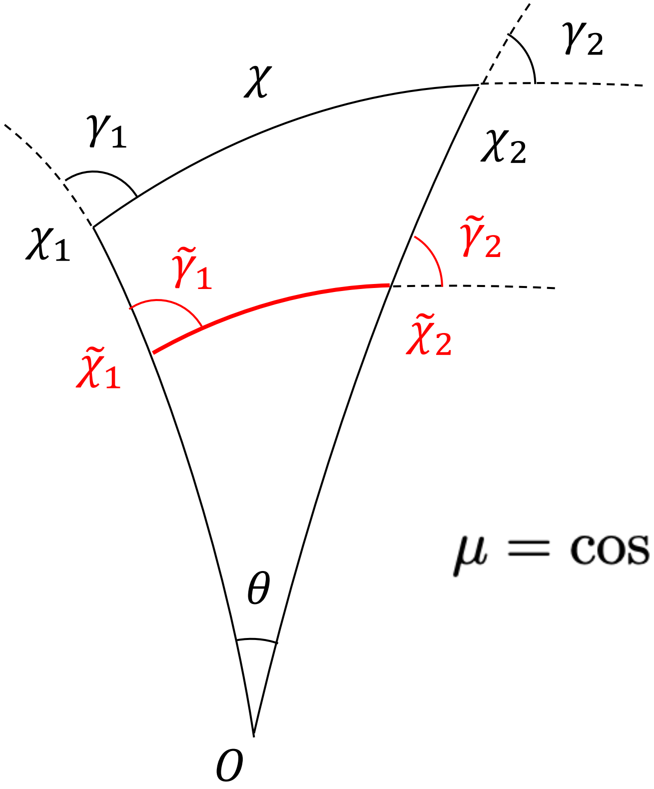

$$r_\parallel E(z) = \tilde{r}_\parallel \tilde{E}(z) \quad \Rightarrow \quad r_\parallel = \alpha_\parallel \tilde{r}_\parallel\,,$$

$$\frac{r_\perp}{D_A(z)} = \frac{\tilde{r}_\perp}{\tilde{D}_A(z)} \quad \Rightarrow \quad r_\perp = \alpha_\perp \tilde{r}_\perp\,,$$

$$\mu = \cos\gamma_1$$

Alcock-Paczynski

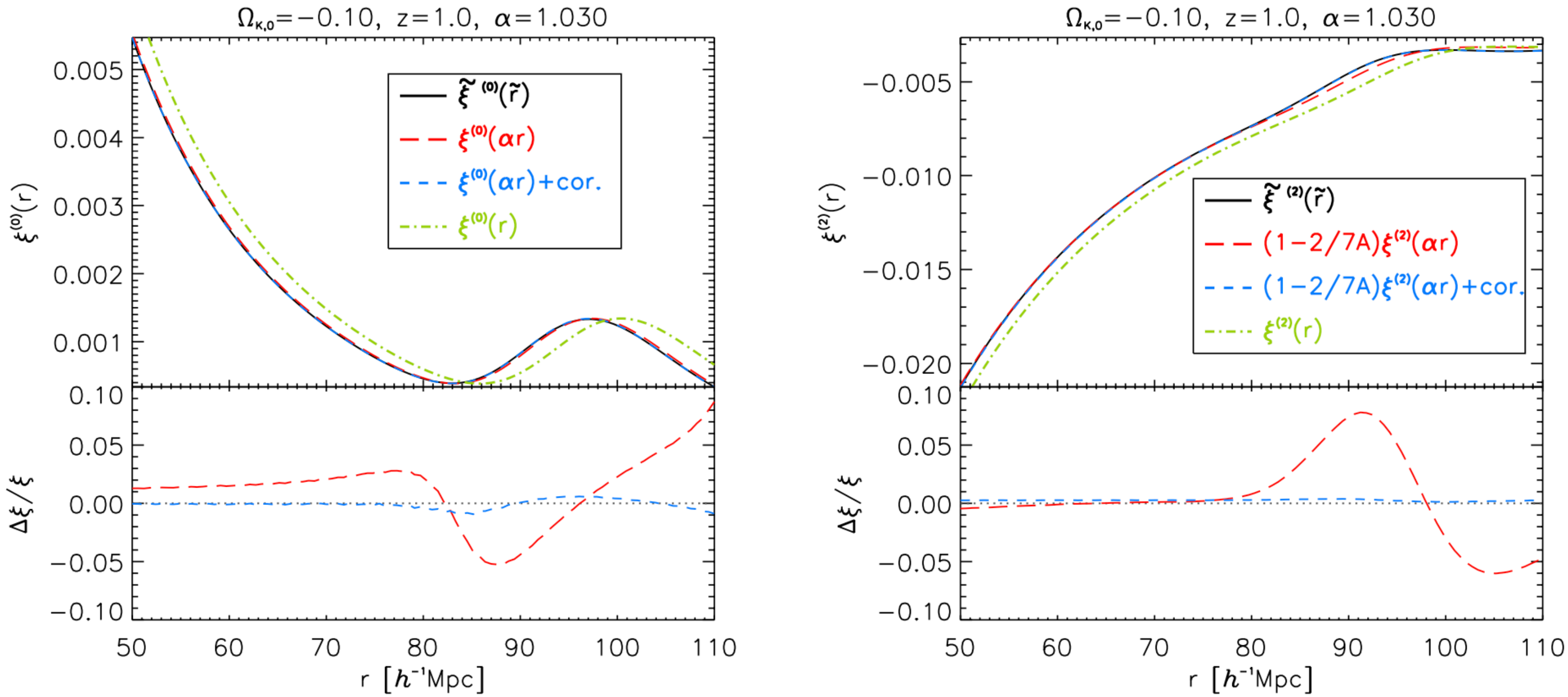

Figure 12. *Top:* AP effect on the monopole (A.16) (left) and quadrupole (A.18) (right). Solid black line shows the true distorted multipoles. Red long-dashed line shows the leading (first) contribution and blue short-dashed line is the correction. Green dot-dashed line shows the multipole without AP effect. Fiducial model: $\Omega_{\mathrm{m},0} = 0.37$, $\Omega_{K,0} = 0$; true model: $\Omega_{K,0} = -0.1$, $\Omega_{\mathrm{m},0} = 0.32$. *Bottom:* Fractional difference relative to true distorted multipoles.